2010

Theoretical Investigation of the structures and stability of gas phase neutral and cationic TixOy clusters.

Baljeet Kaur
Virginia Commonwealth University

Theoretical Investigation of the structures and stability of gas phase neutral and cationic Ti_xO_y clusters

A Thesis submitted in partial fulfillment of the requirements for the degree of Master of Science in Physics / Applied Physics at Virginia Commonwealth University.

by

Baljeet Kaur

M.S. in Physics/Applied Physics
Virginia Commonwealth University, 2010

Director: SHIV N. KHANNA
PROFESSOR, DEPARTMENT OF PHYSICS

Virginia Commonwealth University,
Richmond, Virginia, 23284

May 10, 2010

Acknowledgments

Foremost, I would like to express my sincere gratitude to my advisor Dr. Shiv N.Khanna for his continuous support of my M.S. study and research, for his patience, motivation, immense knowledge and his guidance that helped me in all the time of research and writing of this thesis. I am extremely grateful to my parents and my husband, Manpreet, for all their support and efforts that encourage me to pursue my higher education I would also like to thank all the members of the Khanna research group, for their help during the past two years. I owe my most sincere gratitude to Dr. Arthur Reber and Dr. Debesh Roy for their patience, support and encouragement. I would also like to thank EVERYONE at the VCU Physics Department for all their help and support.

Table of Contents

List of Figures

Page

Abstract

By Baljeet Kaur, M.S.

A thesis submitted in partial fulfillment of the requirements of the degree of Master of Science at Virginia Commonwealth University.

Virginia Commonwealth University, 2010.

Major Director: Shiv N. Khanna, Professor, Department of Physics

Theoretical investigation of the structure and stability of neutral and cationic Ti_xO_y cluster series (where y =2x-1, 2x, 2x+1) have been performed. The lowest lying structures for the neutral clusters are usually found in the singlet state. Generally, in bulk and in the case of the neutral Ti_xO_y clusters, the 2x cluster series is relatively more abundant than the 2x-1 and the 2x+1 cluster series. But in the case of cationic Ti_xO_y clusters, the 2x-1 series is more abundant. To understand the origin of the stability of the $Ti_xO_{2x-1}^+$ clusters, we use density functional theory within the NRLMOL set of codes. Different analyzing factors such as ionization potential, TiO_2 removal energy, oxygen removal energy, binding energy per atom and HOMO-LUMO gap have been used to examine the relative stability of $Ti_xO_{2x-1}^+$ clusters. After analyzing the above criteria, we find that the ionization potential and HOMO-LUMO gap are more reliable, as the low ionization potential of the 2x-1 series generally implies low HOMO-LUMO gap and suggests that the 2x-1 cluster series more likely prefer to remain as cations. To further confirm this, we examine the density of states of Ti_3O_5 and Ti_3O_6 which show a larger HOMO- HOMO-1 gap in case of Ti_3O_5, indicating that the cluster would like to lose an electron for enhancing electronic stability.

Chapter 1: Introduction

1.1 Atomic – Clusters:

Atoms are the primitive building blocks of all the materials found in nature [1-5]. These primitive units can be arranged in different forms and patterns, depending on thermo-dynamical parameters such as temperature and pressure. The properties of the materials depend on the arrangement of these primitive units. The different arrangement of same type of atoms leads to diverse material characteristics. As an example, carbon forms graphite, diamond and C_{60} fullerides structures as shown in Fig.(1.1) below.

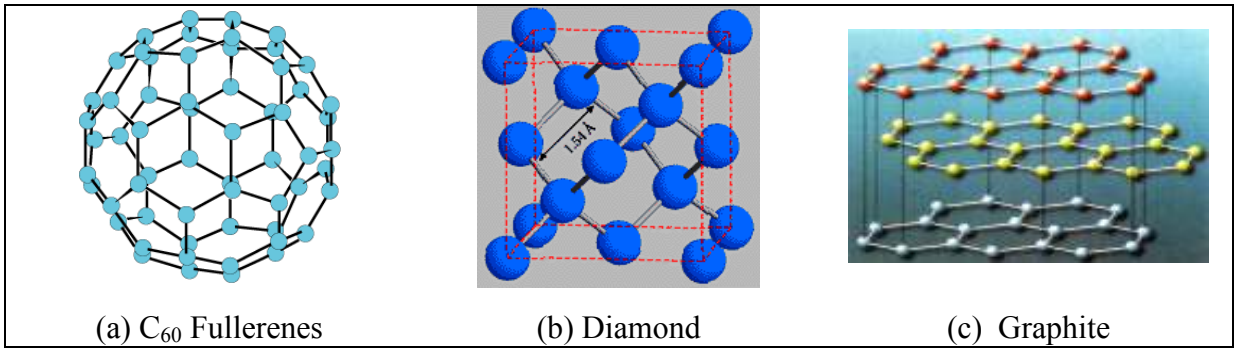

(a) C_{60} Fullerenes (b) Diamond (c) Graphite

Figure (1.1): Shows different arrangement of carbon atoms in C_{60} Fullerenes Diamond and Graphite

Fulleride is a crystal of C_{60} clusters while graphite and diamond are crystals with C atoms as building blocks. Even though all of them are composed of carbon atoms, the superconducting properties of fullerides are different from graphite and diamond. Diamond is one of the hardest known materials and acts as an insulator because of the tetrahedral arrangement of carbon atoms, on the other hand graphite is soft and slippery and has a planar

structure which allow the electrons to move easily in the planes and thus conduct electricity and heat.

Extensive research over the past two decades has shown that new behaviors can emerge when matter is divided into nanometer or sub-nanometer length scale. The physical, chemical, electronic, magnetic and optical properties of the atomic clusters containing two to a few hundred atoms are found to be very different from those of individual atoms or solids. To cite a few examples, while Au is a noble metal, the small clusters of Au are highly effective catalysts for the conversion of CO to CO_2. While bulk Rh is non-magnetic, small clusters of Rh are magnetic. The most exciting aspect of clusters is that the properties are highly size dependent. For example the reactivity of Fe_n clusters have been found to change significantly by the addition of the single atom. This shows that if the materials could be build using atomic clusters as the building blocks, it may be possible to control the properties through judicious choice of primitive clusters.

The most important aspect in cluster science is the stability of the atomic clusters. In 1984, Knight and co-workers observes that the alkali metal clusters with 2, 8, 18, 20, 40, 58, …. are more abundant than the others [1]. These prominent sizes are called the magic numbers. Ekardt and Knight and co-workers also proposed that the stability of the magic clusters could be reconciled with a simple Jellium picture. In Jellium model, the cluster is replaced by the spherical symmetrical potential well, with the positive charge density being uniform inside the sphere and zero outside. The electronic levels in such a potential can be labeled by a radial and angular momentum quantum number , **nl** , much in the same way as in case of the atoms(Note that the potential has a different radial dependence in atoms and it

leads to different combinations of nl). Similar to the case of atoms, the magnetic quantum number takes value from –l, -l+1, …. , 0 , ……, l-1, l and the spin quantum number takes two values of ± ½ . In Fig. (1.2) we schematically show the one electron levels in an H-atom and those in a spherical Jellium (the energy levels in the two systems are not inferred to be the same).

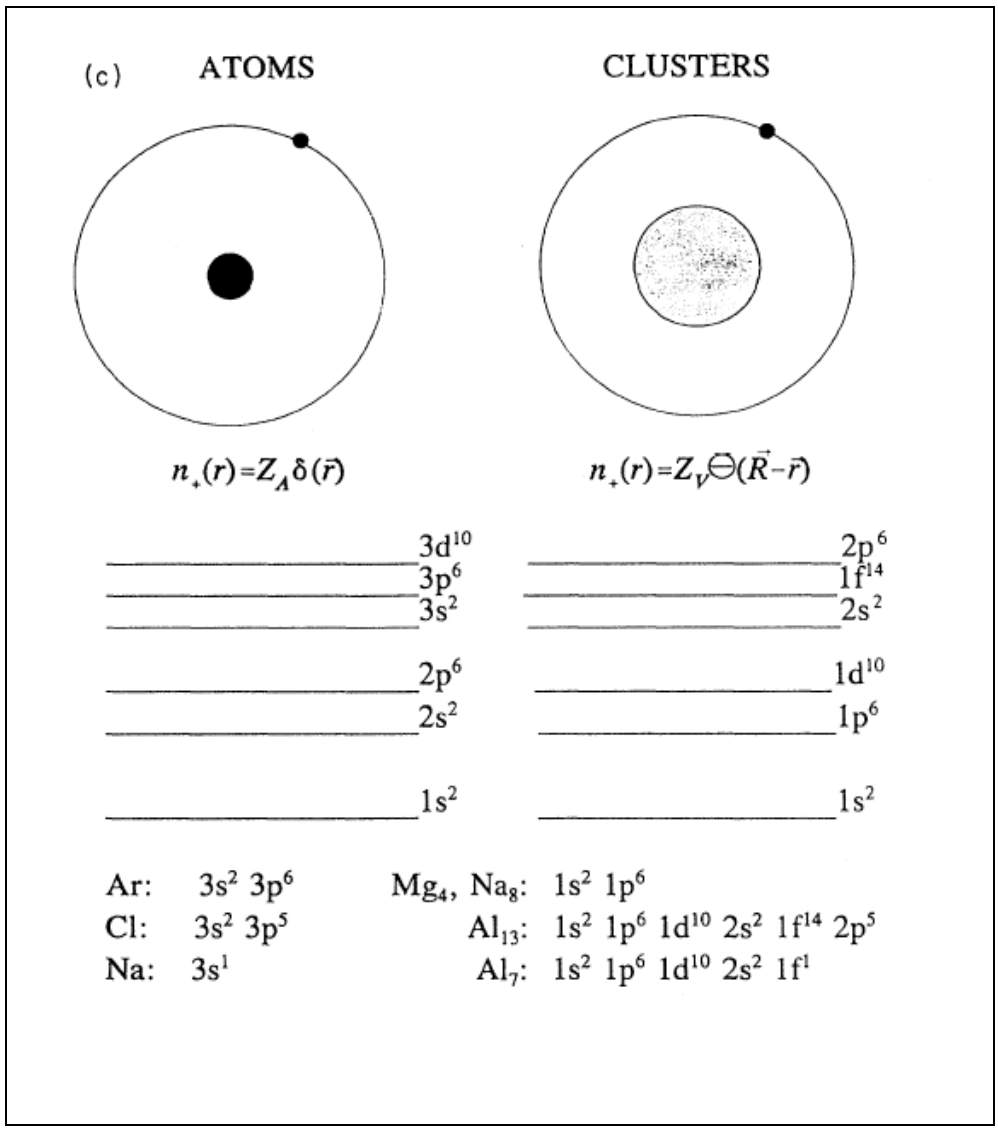

Figure (1.2): Energy levels in atoms and clusters.

Note the ordering $1s^2 1p^6 1d^{10} 2s^2 1f^{14} 2p^6 \ldots$ compared to $1s^2 2s^2 2p^6 3s^2 3p^6 3d^{10} \ldots$ for the H atom. Fairly similar ordering of levels (expect for higher energy levels) is obtained for the harmonic, intermediate and square well forms of the potential, although the spacing between the shells is changed. The key result is that the electronic shell structure is a generic property of the confined nearly free electron gas. It is known that the atomic and molecular systems with filled electronic shells and large gap in the excitation spectrum are more stable. Thus the electronic shell structure governs the stability of the cluster. As the cluster size increases, the extended cluster orbitals tend to condense into highly degenerated shells and other effects begin to contribute to the stability. For example, experiment on sodium clusters containing up to several hundred atoms showed that the major and the minor peaks in the mass spectrum could be reconciled as due to geometric effects. While the major peaks corresponded to the completion of complete icosahedral shell of atoms with the set of twenty minor peaks seemed associated to completion on one of the triangular faces of the growing icosahedral shell. These experiments indicate that at larger cluster size the stability is dominated by the geometric compactness of the clusters. The general conclusion was that the stability of the cluster depends on electronic and geometrical components. While the electronic effect dominates at small sizes, the geometric compactness dominates at larger sizes.

In case of the transition metal clusters, due the existence of opened d shell, the chemical and physical properties of these clusters show remarkable size dependent variations that can not be explained within the jellium model. This presents a tremendous challenge to study experimentally and theoretically the properties of transition metal clusters. But with the rapid

development of experimental and computational techniques it is possible to study these clusters.

1.2 Titanium Oxide Clusters:

In recent years, Titanium oxide clusters have attracted a particular interest due to their potential technological applications as their bulk phase materials, which play an important role as superconductors and catalysts [6-20]. These nanosized titanium oxide clusters possess unusual structural, electronic and optical properties that are quite different from the bulk phase. Titanium oxide has widespread applications because of its low cost, stability and environmental compatibility. For instance, nanosized titanium oxide materials are widely used as photocatalyst for converting solar energy into chemical energy. Titanium oxides also act as a good medium for environmental cleanup through photo-oxidation of the organic pollutants in water and in air. Titanium oxide is also used as a stable white UV proof pigment in sunscreen lotions. Small titanium oxide clusters are also of astro-physical importance due to the relative abundance of elements Ti and O in the interstellar space. It is expected that in the near future, many environmental and energy related issues might be solved by the applications of titanium oxide nano clusters.

Titanium with an electronic configuration [Ar] $4s^2$ $3d^2$ and belongs to group 4B of the periodic table, while oxygen with an electronic configuration of $1s^2$, $2s^2$, $2p^4$ belongs to group 6A of the periodic table. Titanium exhibits different oxidation state in different chemical compounds especially in oxides. The coordination number and the oxidation state of the titanium atom play an important role in the study of the structure and other properties

of titanium oxide clusters. These cluster complexes are very important because of the transition of titanium to different oxidation states, as it leads to clusters with different behaviors e.g metallic, insulating and semi conducting with almost the same constituents.

In nature, bulk titanium oxide exists in three different phases: rutile , anatase and brookite. The rutile phase is considered to be the most common and most stable phase of titanium oxide. Both anatase and brookite transform into rutile phase upon heating. In all the three phases, Ti cations have a coordination number of 6, meaning that each Ti cation is surrounded by an octahedron of 6 oxygen atoms. The oxygen anion has coordination number 3, meaning each oxygen anion is surrounded by three Ti atoms in trigonal planar symmetry. Both rutile and anatase have a primitive tetragonal unit cell with two sides of equal lengths and a third side of different length and all angles are equal to 90 degrees. The brookite on the other hand has a primitive orthorhombic unit cell with all the three sides of unequal lengths and all angles equal to 90 degrees as shown in the Fig.(1.3) below.

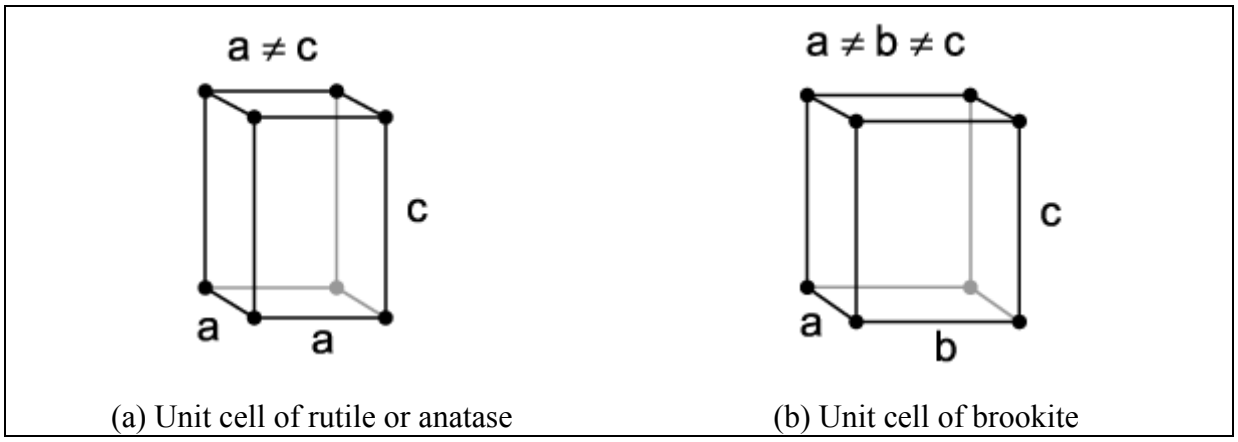

(a) Unit cell of rutile or anatase (b) Unit cell of brookite

Figure (1.3): The tetragonal unit cell of rutile or anatase and the orthorhombic unit cell of brookite.

Before we move to the objectives of this study, let us discuss briefly about the experiment by which the mass spectra is obtained.

1.3 Experimental Details :

A schematic view of the molecular beam apparatus equipped with a reflectron time of flight (TOF) mass spectrometer, used to obtain the mass spectra of Ti_xO_y cationic cluster is shown in Fig (1.4) [21-25].

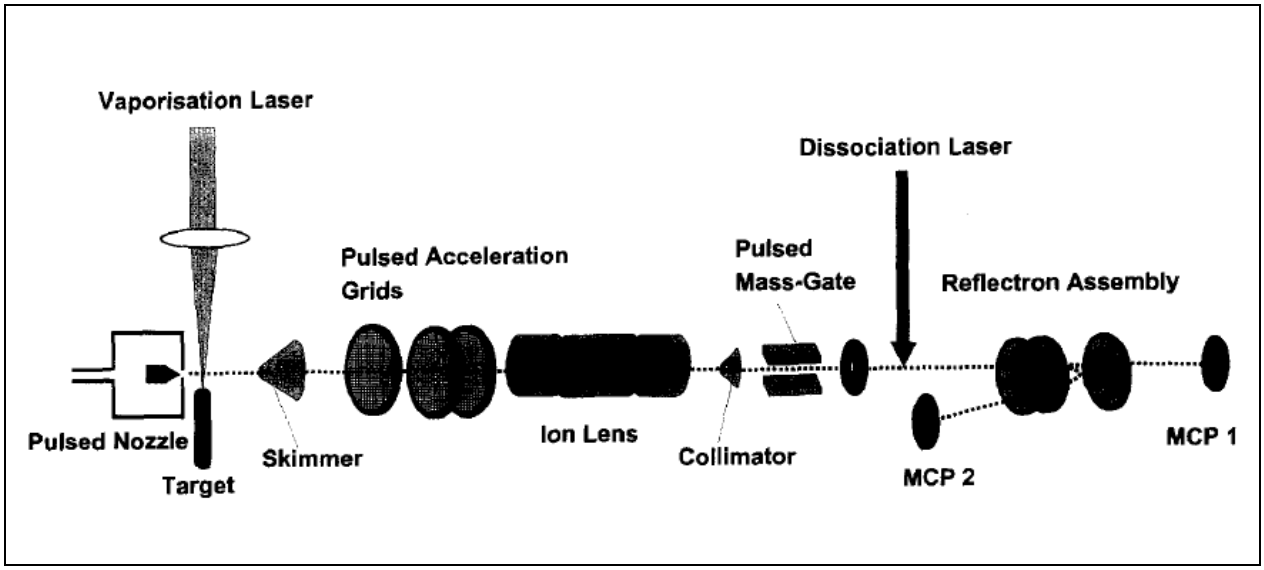

Fig. (1.4): A schematic diagram of the experimental apparatus.

The apparatus consists of three differentially pumped chambers:

(a) **Ablation Chamber:** In this chamber, plasma is produced by the laser ablation of solid rotating Ti rod and cooling obtained from the supersonic expansion of a noble gas. A 10ns pulsed laser beam Nd:YAG at 1064nm or XeCl excimer at 308nm is used for target ablation.

The laser beam is focused on the target surface using a lens with 50 cm focal length. The laser produced plasma is mixed with an expanding O_2 gas pulse provided by piezoelectric nozzle. The Titanium oxide clusters are created via association and dissociation, in the form of molecular beam containing neutral and ionic species.

(b) **Accelation Chamber**: This chamber is separated from the source chamber with a 4mm skimmer. It contains double-field (250V/cm, 925V/cm) pulsed electrode for the TOF analysis of the produced cluster-ions.The first field is formed by two parallel flat grids and is located 14 cm from the formation region. This long field allows us to accelerate the entire ion-packet produced from the source.

(c) **Detection Chamber:** This chamber consists of reflectron assembly. Two micro channel plates (MCP) detectors are used to measure the intensities of the positive ions. The first detector MCP1 is placed along the ion beam and is used to optimize initially the cluster production for maximum signal. While the second MCP2 is placed off axis and is used to obtain the mass spectra of the backward reflected ions from the reflectron assembly. MCP2 output is directly connected to a computer controlled digital storage oscilloscope where the TOF mass spectra are acquired and stored shot by shot. One has to take the average of several single transients to obtain the mass spectra.

1.4 Objectives of this work:

The main objective of this work is to study the stability and the structures of three different series of cationic titanium oxide clusters, obtained by using a infrared (1064nm, 6ns pulse width) laser ablation of pure titanium rod. The typical mass spectrum obtained by Michalis Velegrakis is shown in Fig.(1.5) below [21]:

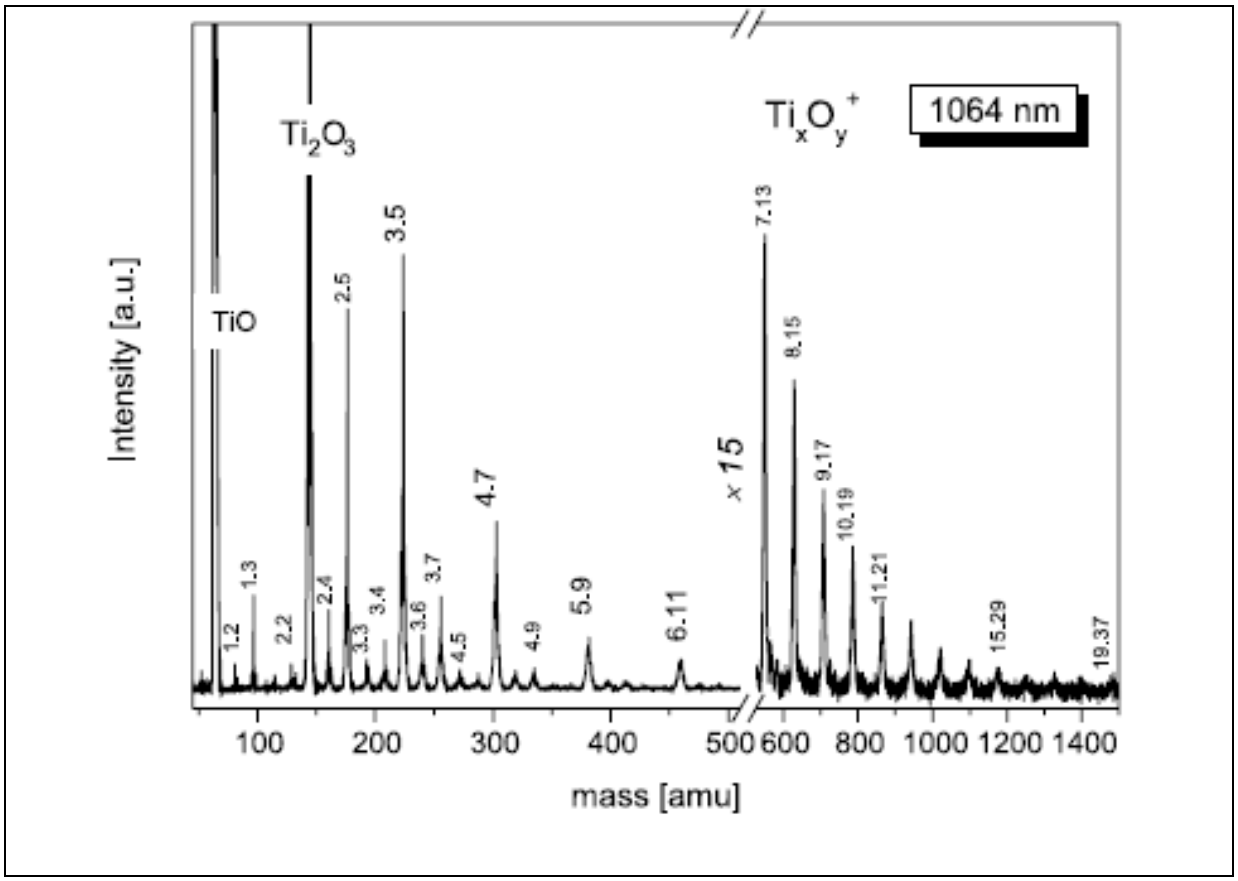

Fig. (1.5): Mass spectra of $Ti_xO_y^+$ clusters produced by the ablation of a Ti target with a Nd:YAG laser (1064 nm, fluence of 2 J/cm^2) in the vicinity of the jet expansion of O_2 gas

Similar series of titanium oxide cationic clusters have been observed in the mass spectra obtained by Yu and Freas [22] by sputtering titanium dioxide power and titanium foil exposed to oxygen and later by others using laser ablation of titanium, TiO_2 and $Ti(SO_4)_2$ targets. All these experiments show that titanium clusters could be distinguish between stoichiometric $(TiO_2)_n^+$ and non-stoichiometeric $Ti_xO_{2x-\delta}^+$ clusters.

According to the valence bond theory, the valence of titanium with configuration [Ar] $3d^2$ $4s^2$ can be at most four. In neutral TiO_2, the oxidation number of Ti is four, provided that oxygen contributes two electrons. Similarly in TiO^+, the oxidation number of Ti is two, thus both TiO_2 and TiO^+ are expected to be the stable species. With these considerations the three series appearing in the mass spectra can be grouped into the formulas: $TiO^+(TiO_2)_n$, $TiO^+(TiO_2)_nO_2$, $(TiO_2)_n$. In all these three series the TiO_2 is the building block of the cluster. The difference between the first and second series is the additional molecular oxygen which could be absorbed in the former series.

Generally, in bulk and in neutral Ti_xO_y clusters, 2x is the most abundant series but in case of $Ti_xO_y^+$ clusters, 2x-1 series has higher intensity and is more stable. The origin of the relative stability of 2x-1 clusters has been examined using different analyzing factors like ionization potential, TiO_2 removal energy, TiO removal energy, oxygen removal energy, binding energy per atom and HOMO-LUMO gap. All these factors have been discussed in detail in chapter 3.

Chapter 2. Theoretical method

2.1 Numerical Methods

The main goal of nearly all numerical quantum chemistry methods [26] is to solve time– independent Schrodinger wave equation (S.W.E). In order to approach this topic, let us start with the standard formulation of S.W.E, which is:

$$\hat{H}\Psi = E\Psi \quad \textbf{(1)}$$

Where $\hat{\mathbf{H}}$ is the Hamiltonian operator, $\mathbf{\Psi}$ is the wave function and **E** is the total energy of the system. For a system with **N** electrons and **M** nuclei, the Hamiltonian is given by:

$$\hat{H} = \frac{-\hbar^2}{2M_A}\sum_{A=1}^{M}\nabla^2{}_A + e^2k\sum_{A=1}^{M}\sum_{B>A}^{M}\frac{Z_AZ_B}{r_{AB}} - \frac{-\hbar^2}{2m_e}\sum_{i=1}^{N}\nabla^2{}_i - e^2k\sum_{i=1}^{N}\sum_{A=1}^{M}\frac{Z_A}{r_{iA}} + e^2k\sum_{i=1}^{N}\sum_{j>i}^{N}\frac{1}{r_{ij}}. \quad \textbf{(2)}$$

where $\mathbf{M_A}$ is the mass of the nucleus, $\mathbf{m_e}$ is the mass of the electron, **k** is the electrostatic constant, $\mathbf{Z_A}$ and $\mathbf{Z_B}$ are the atomic numbers, **e** is the unit charge and r_{AB} , r_{iA} and r_{ij} are the nuclei to nuclei distance, nuclei to electron distance and electron to electron distance respectively .In terms of Atomic Units, where m_e, e, $\hbar$, and k are unity, the above Hamiltonian becomes:

$$\hat{H} = \frac{1}{2M_A}\sum_{A=1}^{M}\nabla^2{}_A + \sum_{A=1}^{M}\sum_{B>A}^{M}\frac{Z_AZ_B}{r_{AB}} - \frac{1}{2}\sum_{i=1}^{N}\nabla^2{}_i - \sum_{i=1}^{N}\sum_{A=1}^{M}\frac{Z_A}{r_{iA}} + \sum_{i=1}^{N}\sum_{j>i}^{N}\frac{1}{r_{ij}}. \quad \textbf{(3)}$$

From time to time, different electronic structure methods have been proposed to solve the S.W.E. given by equation (1).The very first approximation in this field was made by **Born-Oppenheimer** in 1927. In this method the motion of the electron is decoupled from the motion of the nucleus. Since the mass of the nucleus is much greater than the mass of the electron, it is assumed that the electrons are moving in the field of fixed nuclei. This means that kinetic energy of nuclei is zero and the coulomb potential between nuclei is constant and is denoted by C. Thus equation (3) reduces to:

$$\hat{H} = C - \frac{1}{2}\sum_{i=1}^{N}\nabla^2{}_i - \sum_{i=1}^{N}\sum_{A=1}^{M}\frac{Z_A}{r_{iA}} + \sum_{i=1}^{N}\sum_{j>i}^{N}\frac{1}{r_{ij}} \qquad \textbf{(4)}$$

The main consequence of this approximation is that the Hamiltonian is divided into two parts.

$$\hat{H} = \hat{H}_{electron} + \hat{H}_{nuclei} = -\frac{1}{2}\sum_{i=1}^{N}\nabla^2{}_i - \sum_{i=1}^{N}\sum_{A=1}^{M}\frac{Z_A}{r_{iA}} + \sum_{i=1}^{N}\sum_{j>i}^{N}\frac{1}{r_{ij}} + C \qquad \textbf{(5)}$$

Even with Born-Oppenheimer approximation, it is not possible to find the exact solution of S.W.E. The only possible way to solve the S.W.E is to assume that there is no interaction between electrons (the electron to electron potential is zero) and thus we can separate the Hamiltonian and wave function for the individual electrons. However, even for the simplest case the result of this approach leads to high deviation from the experimental results .This indicates that in reality the electron–electron interactions are non-zero. In 1928, Hartree introduced another approximation called Hatree method to solve the S.W.E. In this method N electron wave function is approximated by the product of N one electron wave function and is given by:

$$\psi(r_1 s_1, r_2 s_2, \ldots\ldots r_i s_i) = \psi(r_1 s_1)\,\psi(r_2 s_2,)\ldots\ldots\psi(r_i s_i) \quad \textbf{(6)}$$

In this approximation, the electron does not interact with other electron on one-one basis, but with the averaged density of the electrons. This weighted electron potential is given by:

$$V_{\text{interaction}} = \frac{1}{2}\sum_i \sum_{j\neq i} \int d\vec{r}_i d\vec{r}_j \frac{\left|\psi_i(\vec{r}_i)\right|^2}{\left|\vec{r}_i - \vec{r}_j\right|} \left|\psi_j(\vec{r}_j)\right|^2 \quad \textbf{(7)}$$

Using the above interaction potential, we can find the expected energy of the system which is given by:

$$E = \left\langle \psi \middle| \hat{H} \middle| \psi \right\rangle = \sum_i \int \psi_i^*(\vec{r}_i)(-\frac{1}{2}\nabla^2 - \sum_{A=1} \frac{Z_A}{r_{iA}})\psi_i(\vec{r}_i) d\vec{r}_i + \frac{1}{2}\sum_i \sum_{j\neq i} \int d\vec{r}_i d\vec{r}_j \frac{\left|\psi_i(\vec{r}_i)\right|^2}{\left|\vec{r}_i - \vec{r}_j\right|} \left|\psi_j(\vec{r}_j)\right|^2 \quad \textbf{(8)}$$

It is possible to split the above equation into N single particle equations, which are much easier to handle. Hartree method allows for the S.W.E to be solved by the iterative process. In this process we start with an initial guess for $\mathbf{V_{int}}$ and used to compute the wave functions $\mathbf{\Psi_i}$ and the energy E of the system. From the computed wavefunctions, a new $\mathbf{V_{int}}$ can be computed, for use in the next iteration. The S.W.E is then solved, until convergence in the energy is reached.

Hartree's method work reasonably well for atoms. For instance when this method is applied to He atom, there is only 1.4% deviation from the experimental value. Although this method provide a great foundation on numerically approximating many body problems, but still it has some limitations. In Hartree method, the probability of finding an electron at a particular point in space is independent of the probability of finding any other electron at that point. This indicates that the electrons behave independently of each other, however, we expect the electrons to affect each other via coulomb repulsion.

Hartree method requires that the specific electrons have been assigned to specific orbitals, thus violates the Pauli exclusion principle, that treats the electrons as indistinguishable.

To solve the problems in the wave function which plagued the Hartree method, Fock in 1930 proposed another approximation called "Hartree-Fock" method. In this approximation the total wave function of the N-electron system is approximated by an antisymmetrized product of N one electron wavefunction. This product is represented by the Slater determinant and is given by:

$$\psi_{SD} = \frac{1}{\sqrt{N!}} \begin{vmatrix} \chi_1(\vec{x}_1) & \chi_2(\vec{x}_1) & \dots & \chi_N(\vec{x}_1) \\ \chi_1(\vec{x}_2) & \chi_2(\vec{x}_2) & \dots & \chi_N(\vec{x}_2) \\ . & . & . & . \\ \chi_1(\vec{x}_N) & \chi_2(\vec{x}_N) & \dots & \chi_N(\vec{x}_N) \end{vmatrix} \quad \textbf{(9)}$$

where,

$$\chi(\vec{x}) = \phi(\vec{r})\sigma(s), \quad \sigma = \alpha, \beta$$

are called the "spin – orbitals" and are composed of both spacial $\phi(\mathrm{r})$ and one of the spin functions α or β components of the electron $\sigma(s)$.

At this point we must introduce the variational principle.The variational principle states that the expectation value for the Hamiltonian operator $\hat{\mathrm{H}}$ in the state ψ_{trial} will yield an energy E_{trial} that would be an upper bound to the ground state energy, i.e.

$$\langle \psi_{trial} | \hat{H} | \psi_{trial} \rangle = E_{trial} \geq E_0 = \langle \psi_0 | \hat{H} | \psi_0 \rangle \quad \textbf{(10)}$$

Thus the function that gives the lower state energy is ψ_0 and the energy will be the ground state energy E_0. Using variational principle the H-F equation becomes:

$$E_{HF} = \left\langle \psi_{SD} \middle| \hat{H} \middle| \psi_{SD} \right\rangle = \sum_i \epsilon_i + \frac{1}{2}\sum_{i=1}^{N}\sum_{j=1}^{N}(\hat{J}_{ij} - \hat{K}_{ij}) \quad \textbf{(11)}$$

where,

$$\epsilon_i = \int \chi_i^*(\vec{x}_i)(-\frac{1}{2}\nabla^2 - \sum_{A=1}\frac{Z_A}{r_{iA}})\chi_i(\vec{x}_i)d\vec{x}_i$$

$$J_{ij} = \int d\vec{x}_i d\vec{x}_j \frac{|\chi_i(\vec{x}_i)|^2 |\chi_j(\vec{x}_j)|^2}{r_{ij}}$$

$$K_{ij} = \int d\vec{x}_i d\vec{x}_j \frac{\chi_i^*(\vec{x}_i)\chi_j(\vec{x}_j)\chi_j^*(\vec{x}_j)\chi_i(\vec{x}_j)}{r_{ij}}.$$

where J_{ij} is called the Coulomb integral and K_{ij} is called the exchange integral. Hartree-Fock theory is also referred to as an independent Particle model or a "mean field theory" because each electron moves independently of all the others except that it feels the Coulomb repulsions due to the "average" position of all the electrons and also exchange interaction due to anti-symmetrization.

Eventhough, HF approximation is a huge improvement from Hartree, where in anti-symmetrization and exclusion principle are correlated, there are some limitations to this approach. HF method neglects electron correlation between the electrons of anti-parallel spin. This neglect is implicit in the use of single SD wavefunction. This calls for the replacement method, the density functional theory.

2.2 Density Functional Theory

Density Functional Theory [26-28] is one of the most successful quantum – mechanical approach to matter in which instead of wavefunction we use an electron density $\rho(r)$ as a variational parameter. This idea was first proposed in 1964 by Hohenberg and Kohn, which states that it is possible to calculate any ground state property of the system through the knowledge of only ground state electron density. This means that any ground state property of the system is the **functional** of electron density.

A functional is defined as a function whose argument is also a function. Functional needs a function as input but delivers a number as output. A functional is described by the square bracket [ ] that surrounds the function it depends on. For example, E [ρ(r)] represents functional dependence of energy E on electron density, which is a function of position coordinate r.

There are four sub-statements of Hohenberg and Kohn (HK) theorem, which are:

1. The ground state expectation value of any observable A is a functional of the ground state density ρ_0 and is given by:

$$A_o = \left\langle \psi(\rho_0) \middle| \hat{A} \middle| \psi(\rho_0) \right\rangle \quad \textbf{(12)}$$

2. The functional that delivers the ground state energy of the system, delivers the lowest energy E_0 only and only if the input density is truly ground state density ρ_0 and is given by :

$$E_0 = \left\langle \psi(\rho_0) \middle| \hat{H} \middle| \psi_0 \right\rangle \; E_0 = \left\langle \psi(\rho_0) \middle| \hat{H} \middle| \psi_0 \right\rangle \quad \textbf{(13)}$$

3. The non-universal potential functional V[n] is given by:

$$V[n] = \int d^3 r \rho(\vec{r}) v(\vec{r}) \quad \textbf{(14)}$$

Ones the system is specified, i.e external potential v(r) is known, the functional V[n] is known explicitly.

4. The external potential v(r), is a unique functional of the ground state density ρ(r). Thus if we know external potential we can determine the complete Hamiltonian and therefore all the excited states of the system.

Out of the above sub-statements of DFT, the fourth statement only holds if DFT is formulated in terms of charge density, but if we include the spin and current densities than in that case the densities still determine the wavefunctions, but fails to determine the corresponding potentials. This shows that HK theorem is not an efficient way of implementing DFT.

In 1965, Kohn and Sham introduced another approach of implementing DFT in which the electron density is represented as if it were derived from a single Slater determinant with ortho-normal orbitals. The density of the electron is given by:

$$\rho(\vec{r}) = \sum_{i=1}^{N} \left| \phi_i(r) \right|^2 \quad \textbf{(15)}$$

where ϕ_i .represents the single electron orbital.

The energy of the electron, using Kohn-Sham equations is given as:

$$E_e = T[\rho(r)] + \int V_{ext}(r)\rho(r)dr + \int V_c(r)\rho(r)dr + E'_{xc}[\rho(r)] \quad \textbf{(16)}$$

where T is the kinetic energy of the system, $\mathbf{V_{ext}}$ is the external potential (due to nuclei in the system), $\mathbf{V_c}$ is the coulomb interaction term and $\mathbf{E_{xc}}$ is the exchange and correlation energy terms. All these terms are the functional of the electron density. It is the last term $\mathbf{E_{xc}}$, what sets DFT apart from the Hartree and Hartree – Fock method.

Many methods have been proposed to handle the exchange correlation between electrons. The first notable approach was the Local Density Approximation (LDA).It is based on homogeneous electron gas in which the total electron density ρ(r) , is constant in space. The exchange correlation term in LDA is given by:

$$E_{xc}^{LDA} = \int dr \rho(r) \varepsilon_{xc}(\rho(r)) \qquad \textbf{(17)}$$

LDA approach has limitation, that it cannot be applied to the spin polarized system.This limitation was overcome by the Local Spin Density Approximation (LSDA) that treated the spin up and spin down electrons separately.The exchange correlation term becomes:

$$E_{xc}^{LSDA}[\rho\uparrow, \rho\downarrow] = \int dr \rho(r) \varepsilon_{xc}(\rho\uparrow(r), \rho\downarrow(r)) \qquad \textbf{(18)}$$

Any real system such as atoms, molecules, clusters and solids are inhomogeneous in space where the electrons are exposed to specifically varying electric fields, thus show the variation in the electron density. Both LDA and LSDA do not take into account the variations in the electron density. This leads to the more commonly accepted functional known as Generalized Gradient Approximation (GGA).The three most important GGA functional used are developed by Becke 88 [B88], Perdew- wang [PW91], and Perdew, Burke, Ernzerhof (96) [PBE].

Like Hartree method, the DFT approach also based on iterative process to solve many-body S.W.E .We start with the electron density ρ(r), and compute the electron wavefunctions. From the wavefunction we can solve the energy of the system. We have to go through the number of iterations, until there is no significant variation in energy of the system. At this point the convergence has been reached and the corresponding energy is called the ground state energy.

2.3 Computational Software Package:

This work presents details on the theoretical investigation on the structures and stability of the neutral and cationic Ti_xO_y clusters, performed by using the density functional theory within the code of NRLMOL. This Naval Research Molecular Orbital Library (NRLMOL) code is developed by Mark Pederson and collaborators. NRLMOL uses Gaussian function to form the basis set it uses for its calculations of the wavefunction. The default basis set for NRLMOL has been specifically optimized for the PBE exchange-correlation functional. NRLMOL is based on the Kohn-Sham formulation of DFT and solves Kohn-Sham equations by expressing the Kohn- Sham orbitals as a linear combination of the Gaussian orbitals. NRLMOL perform calculations involving all the electrons (core electrons + valence electrons), and so does not neglect any electron contribution to the system. NRLMOL uses the point group symmetry of the molecules in the efficient manner.

CHAPTER 3 : RESULTS

The motivation of this work is to understand the origin of the large gas phase abundance of the $Ti_xO_{2x-1}^+$ clusters, and to analyze the stability and electronic structure of the neutral and cationic Ti_xO_y clusters.We will focus on three series of clusters, the series where y = 2x-1, because of the large abundance in the cationic mass spectra, y=2x which corresponds to the bulk stoichometry, and y=2x+1, as it is also observed as cations in the mass spectra. As bulk titanium-oxide, and nanoparticles of TiO are found to have the stoichometry of Ti_xO_{2x}, most previous work on clusters has focused on the Ti_xO_{2x} series. In this study, we will first find the lowest lying structures of the neutral and cationic Ti_xO_{2x-1}, Ti_xO_{2x} and Ti_xO_{2x+1} clusters where x=1-5. Second, we will analyze the stability of these clusters using a variety of different energetic criteria like ionization potential, TiO_2 removal energy, TiO removal energy, oxygen removal energy, binding energy per atom and electronic properties such as the HOMO-LUMO gap (Highest Occupied Molecular Orbital-Lowest Unoccupied Moelcular Orbital). Third, we will consider the success of different criteria in explaining the stability of different neutral and cationic Ti_xO_y clusters. Finally, we will examine the electronic structure of the clusters to look for the root causes of the trends in stability.

The geometries of the lowest lying structures for three different series of neutral and cationic Ti_xO_y clusters, where the series correspond to y = 2x-1, y=2x and y=2x+1 clusters, have been obtained by using the NRLMOL set of density functional codes [29-31], as described in Chapter 2. The resulting ground state geometries where x=1-5 are shown in

Figure (3.1) for the neutrals and in Figure (3.2) for the cations. The Ti atoms are shown in aqua and the oxygen atoms are shown in red.

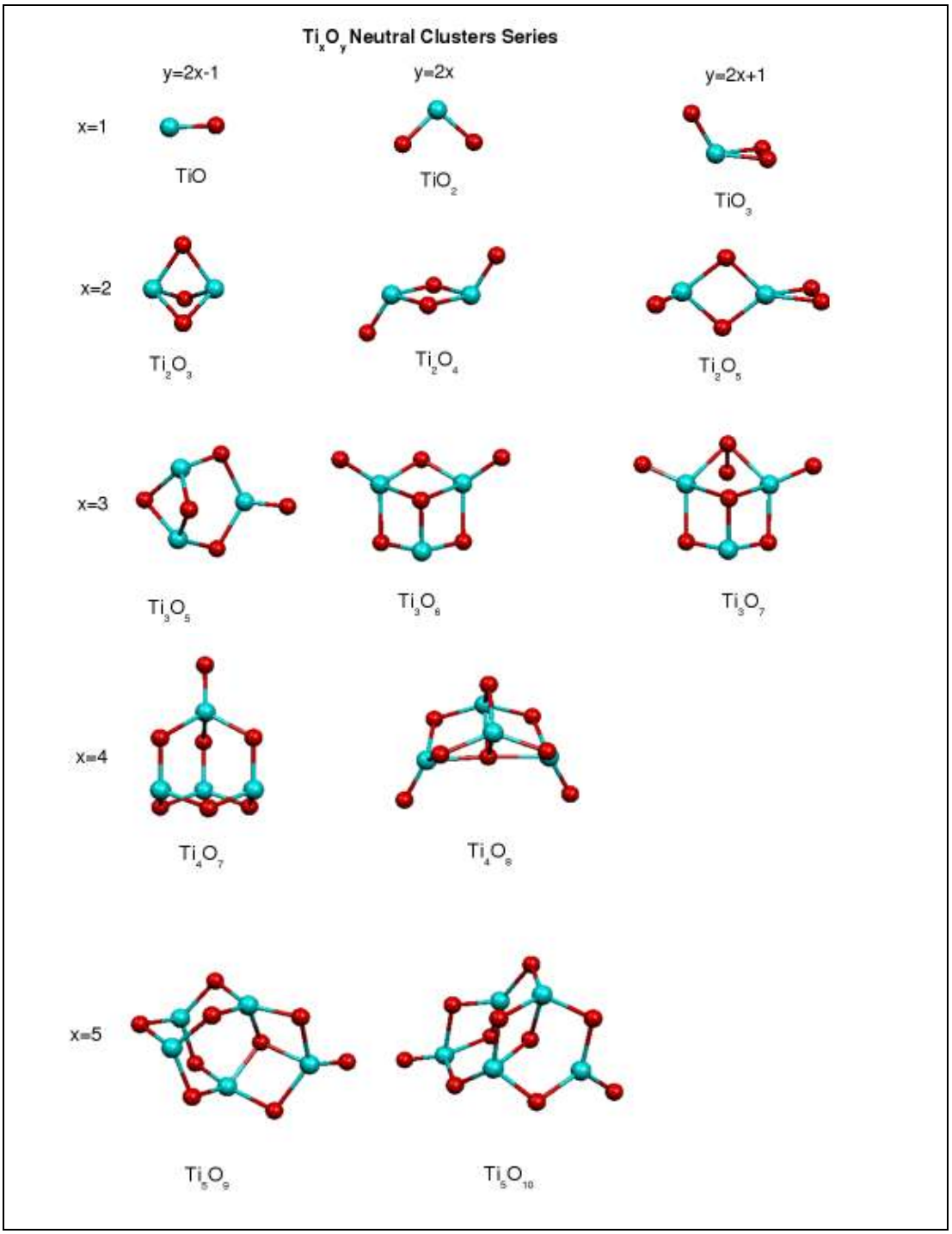

Fig (3.1) : Lowest lying structures for Ti_xO_y cluster series.

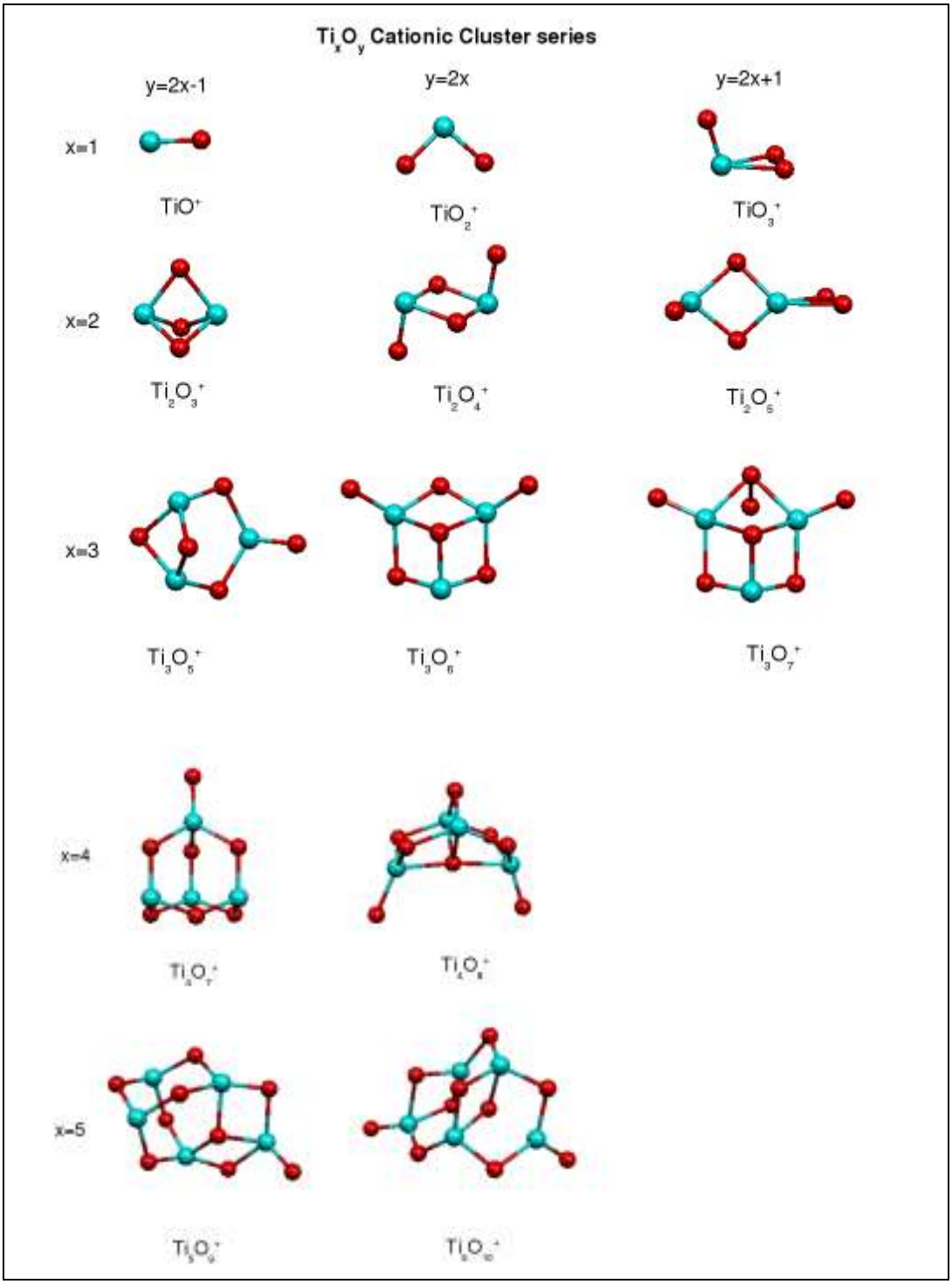

Fig (3.2) : Lowest lying structures for $Ti_xO_y^+$ cluster series

In general, the Ti-O bond is much stronger than Ti-Ti bonds and O-O bonds, so nearly all of the bonds are Ti-O bonds. Oxygen generally prefers to be divalent but in the Ti_xO_y clusters the oxygen shows a variety of valences, such as terminal oxygen which is bound only to a single titanium atom, divalent bridging oxygen, and as the size increases oxygen atoms exhibits trivalent and tetravalent character. As shown in the above figures, the cationic clusters keep the same geometries as their neutral parents, with small changes in bond lengths and bond angles. Let us discuss the structures and bond length in the three different neutral and cationic cluster series.

(3.1) Ti_xO_{2x-1} neutral and cationic cluster series:

The lowest lying structures for Ti_xO_{2x-1} neutral cluster series are always found in the singlet ground state while for Ti_xO_{2x-1} cationic cluster series the lowest lying structure is found in the doublet state. The starting member of this series is TiO, which has linear structure. For Ti_2O_3, the structure is like rhombic unit with three bridging oxygen atoms. Ti_3O_5 shows hexagonal ring like structure with trivalent bridging oxygen and one terminal oxygen atom. As we move to the next member of the series we see that Ti_4O_7 has a bulk like structure with six bridging and a single terminal oxygen atom. For Ti_5O_9 we have a double-cage like structure with eight bridging oxygen atom and one terminal-oxygen atom. In this series, the terminal Ti – O bond is almost of constant length (~ 1.64 Å and 1.61 Å) for neutral and cationic clusters respectively. On the other hand the bond length for bridging Ti – O bond varies between 1.76 Å to 2.04 Å for the neutral clusters and between 1.73 Å to 2.02 Å for cationic clusters.

(3.2) Ti_xO_{2x} neutral and cationic cluster series:

The lowest lying structures for the Ti_xO_{2x} neutral series is also found in the singlet ground state and for Ti_xO_{2x} cationic cluster the lowest lying energy state is found in the doublet state. The starting member of this series is TiO_2, which has bent structure. For Ti_2O_4, the lowest lying structure is a rhombic unit with two terminal oxygen atoms. For Ti_3O_6, the structure is a hexagonal ring with four bridging oxygen and two terminal oxygen atoms. In this structure one bridging oxygen atom is trivalent. As we move to Ti_4O_8, the structure is cage like with one tetravalent bridging oxygen and two terminal oxygen atoms. The terminal Ti–O bonds for this series are almost of constant length (1.64 Å and 1.71 Å) for neutral and cationic clusters respectively. In the case of neutral clusters the Ti–O length varies between 1.76 Å to 2.04 Å and for the cationic clusters it varies between 1.75 Å to 2.01 Å.

(3.3) Ti_xO_{2x+1} neutral and cationic cluster series:

As in the previous two series the lowest lying structures are found in singlet ground state for neutral clusters and in doublet state for cationic clusters. The starting member of this series is TiO_3, which has one terminal oxygen atom and one peroxo group (O^p -O^p). For Ti_2O_5, we have a rhombic unit with one peroxo group and one terminal oxygen atom. For this series the peroxo group has bond length approximately equal to 1.47 Å for neutrals and about 1.37 Å for cationic clusters. The terminal Ti - O bond length is ~ 1.64 Å for both the neutral and cationic clusters. The Ti – $O^{(p)}$ bond length is ~ 1.85 Å for the neutral clusters and ~1.96Å for the cationic clusters. The presence of the peroxo group suggests that the loss of

O_2 is a likely mechanism for fragmentation, and that the binding of O_2 to the Ti^xO_{2x-1} is a likely formation mechanism.

Now that we have the lowest lying structures and the corresponding energy values, we can analyze the energetics of these clusters to understand stability and the mass spectra shown in Fig (1.5) for three different Ti_xO_y cationic clusters series. This also allows us to evaluate different criterion for predicting the gas phase abundance of $Ti_xO_{2x-1}^+$ clusters, such as the ionization potential, the TiO_2 removal energy, oxygen removal energy, the binding energy per atom, and the HOMO-LUMO gap. Also, these criterion may be applied to the neutral clusters, as in bulk and in neutral clusters the stability of Ti_xO_{2x} clusters is greater than $Ti_xO_{2x+1}$and Ti_xO_{2x-1} clusters, but in case of cationic clusters Ti_xO_{2x-1} cluster series has greater stability. To understand this we applied different analyzing factors.

Let us discuss these factors one by one in detail:

(1): Ionization Potential: Fig (3.3) below shows the ionization potential of the Ti_xO_y clusters. In plasma where the clusters are born, both the neutral and charge clusters are created, but in the mass spectra only charged clusters are observable and the neutral ones are invisible. In our case the mass spectra shows cationic clusters, so the ionization potential seems to be a reliable criterion to analyze the energetic and stability of these cationic clusters. There is a competition between different cationic and neutral clusters and clusters which have low ionization potentials are more likely to exist as cations.

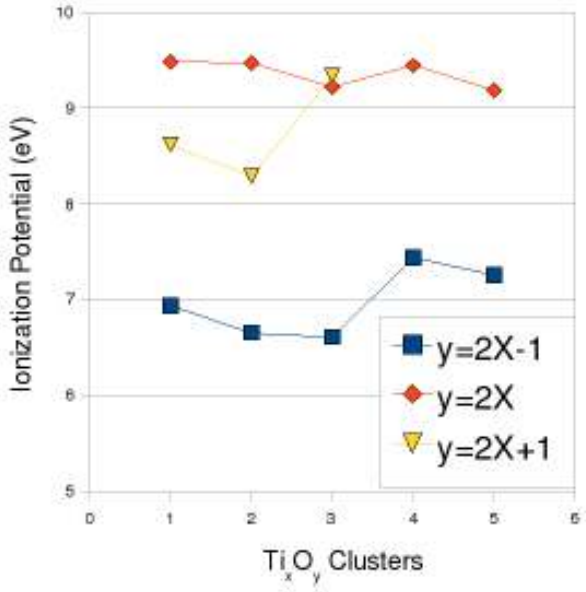

Fig (3.3): Ionization Potential for Ti_xO_y clusters

Let us consider the collision reaction between $Ti_3O_6^+$ and Ti_3O_5:

$$\mathbf{Ti_3O_6^+ + Ti_3O_5 \rightarrow Ti_3O_5^+ + Ti_3O_6 + 2.62\ eV} \qquad \mathbf{(1)}$$

The above reaction is highly exothermic. The ionization potential of Ti_3O_6 is higher than Ti_3O_5 cluster, so Ti_3O_5 is more likely to exist as cation. The *ab initio* quantum-chemical calculations on the stability and structure of these Ti_xO_y clusters indicate that neutral Ti_xO_{2x-1} clusters possess lower ionization potentials (7 eV) in comparison to Ti_xO_{2x} clusters (9.5 eV) and Ti_xO_{2x+1} clusters (9 eV). The higher the ionization potential, the more stable the neutral cluster and it is less likely to convert into the cationic cluster. This shows that Ti_xO_{2x-1} cationic clusters have more stability than Ti_xO_{2x+1} and Ti_xO_{2x} cationic cluster series, or at least are more likely to form in an experiment. This trend can be easily visualized from fig (3.3).

(2) TiO_2 Removal Energy: Besides ionization potential the TiO_2 removal energy criterion can also be used to compare the relative stabilities of Ti_xO_y cluster series**.** Fig (3.4) & (3.5) below show the TiO_2 removal energy for the neutral and cationic Ti_xO_y clusters.

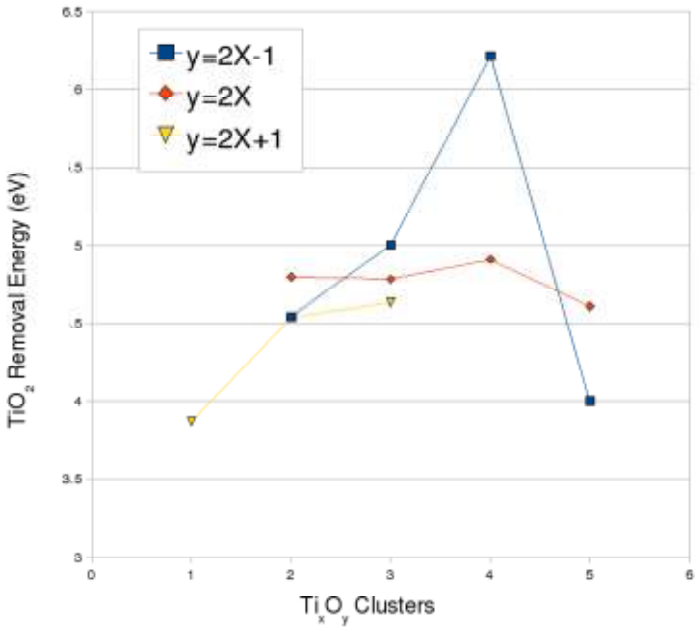

Fig. (3.4) : TiO_2 Removal Energy for Ti_xO_y cluster series

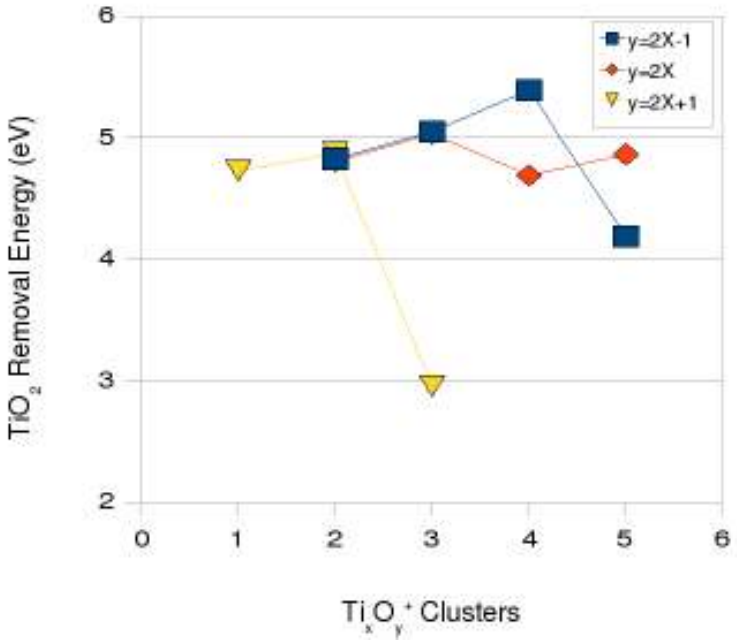

Fig. (3.5) : TiO_2 Removal Energy for $Ti_xO_y^+$ cluster series

The general equation for TiO_2 removal is given as :

$$\mathbf{R.E.\ (TiO_2) = E\ (Ti_{x-1}O_{y-2}) + E\ (TiO_2) - E\ (Ti_xO_y)} \qquad \mathbf{(2)}$$

As seen in Fig (3.4) &(3.5), both the neutral and cationic Ti_xO_y clusters show sharp peaks corresponding to Ti_4O_7 and $Ti_4O_7^+$ clusters indicating that these are the most stable clusters in that series. Also there is a considerable amount of decrease in TiO_2 removal energy as we move to Ti_5O_9 and $Ti_5O_9^+$ clusters. This suggests that Ti_4O_7 may be a "magic", or highly stable cluster. If we look at the mass spectra we see that the intensity of $Ti_4O_7^+$ is higher than $Ti_5O_9^+$ but is lower than $Ti_3O_5^+$ clusters. The cluster source used in Fig.(1.4) appears to have trouble making larger clusters, and the cluster abundance decreases with size, so it is not clear if the $Ti_4O_7$is particularly stable or not. The TiO_2 criterion is not very useful for

comparison between the three different cationic cluster series because every time you remove one TiO_2 unit you stay in the same series. So the TiO_2 removal energy is useful in comparing the stability within the same series, but not between series.

(3) **Oxygen removal energy:** Fig (3.6) & (3.7) below show the oxygen removal energy for neutral and cationic Ti_xO_y clusters. This criterion is used to compare the stability of neutral and cationic Ti_xO_{2x} and Ti_xO_{2x+1} cluster series.

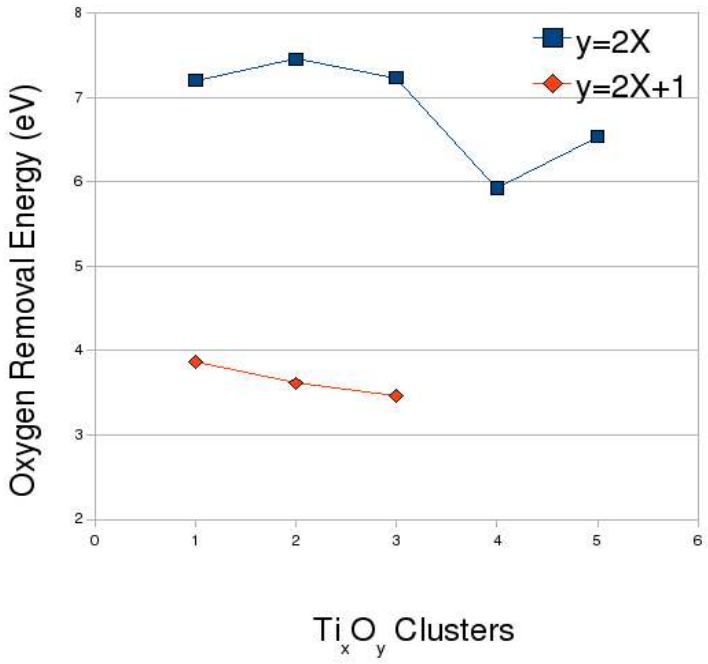

Fig.(3.6) Oxygen Removal Energy for TixOy clusters

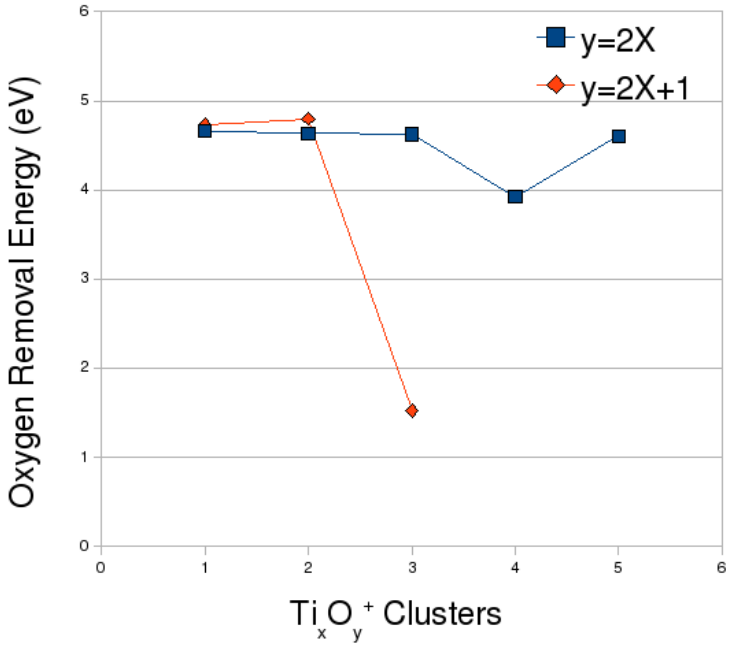

Fig.(3.7) Oxygen Removal Energy for $TixOy^+$ clusters

The general equation for oxygen removal is given as:

$$O(R.E.) = E\,(\,Ti_xO_{y-1}) + E\,(O) - E\,(Ti_xO_y) \qquad (3)$$

In case of neutral Ti_xO_y clusters the oxygen removal is higher for Ti_xO_{2x} series than Ti_xO_{2x+1} series indicating that Ti_xO_{2x} series has higher stability than Ti_xO_{2x+1} clusters with respect to the loss of one oxygen atom from terminal Ti-O bond during collision with other species. This means that in collisions in which the clusters exchange O atoms, Ti_xO_{2x} clusters are more likely to retain their O atoms then Ti_xO_{2x+1} clusters. So the Ti_xO_{2x+1} series are more likely to exit as cations as compared to Ti_xO_{2x} series.As we look at the plot for the cationic clusters we see a considerable amount of decrease in energy in case of $Ti_3O_7^+$ as compared to $Ti_2O_5^{+.}$ This indicates that $Ti_2O_5^+$ is more stable than $Ti_3O_7^+$ cluster. If we look at the mass

spectra we see a large peak corresponding to $Ti_2O_5^+$.This criterion also has some limitations as we are just comparing the two series not all three of them.

At this point we note that the removal O_2 is the favored fragmentation mechanism for the $Ti_xO_{2x+1}^+$ clusters. In Eq. (4) we show a likely reaction.

$$\mathbf{Ti_3O_7^+ + 1.006\ eV \rightarrow Ti_3O_5^+ + O_2} \qquad \mathbf{(4)}$$

This is because the $Ti_3O_7^+$ has an intact O-O bond suggesting that O_2 is a good leaving group. The reverse process is also possible, and the binding O_2 to the more stable $Ti_3O_5^+$ may be the origin of the greater abundance of $Ti_3O_7^+$ than $Ti_3O_6^+$, as excess O_2 is flowed into the source in mass spectra described in Fig (1.4)

(4) TiO Removal Energy: Fig (3.8) & (3.9) below show the TiO removal energy for the neutral and cationic Ti_xO_y clusters.

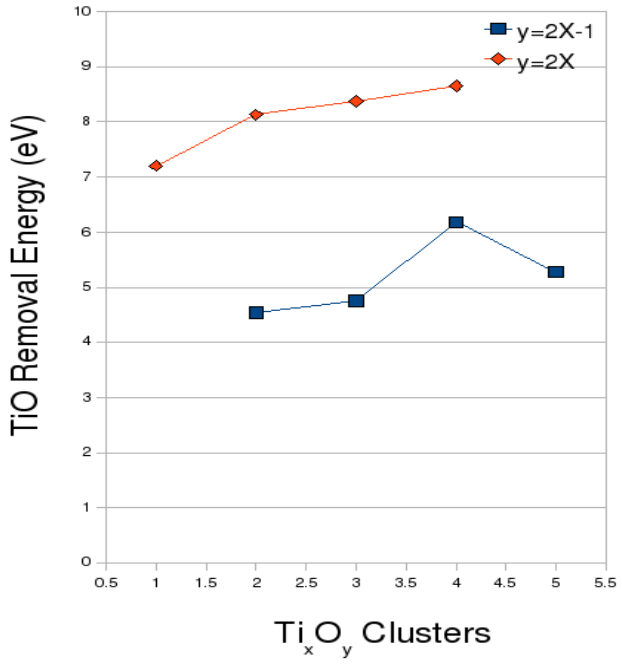

Fig (3.8): TiO Removal Energy for Ti_xO_y cluster series

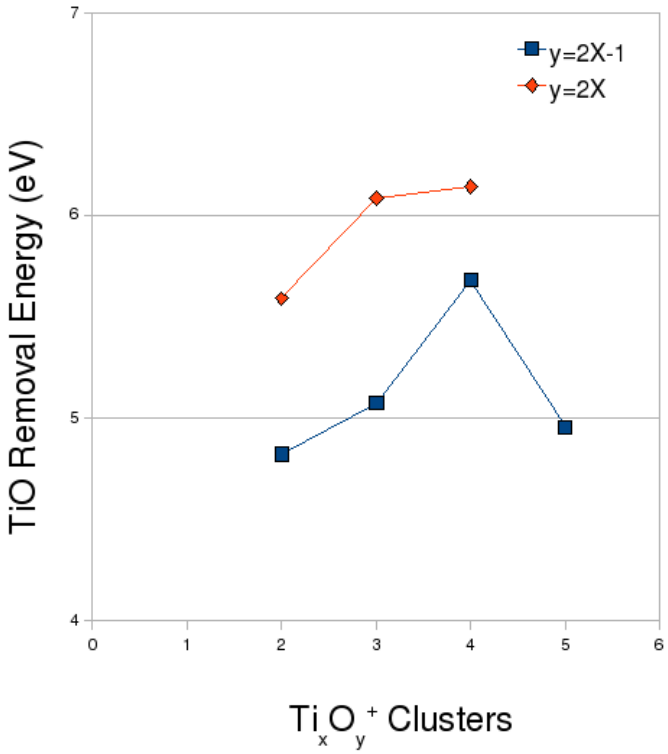

Fig (3.9) TiO Removal Energy for $Ti_xO_y^+$ cluster series

The general equation for TiO removal is given by:

$$\textbf{R.E. (TiO)} = \textbf{E } (Ti_{x-1}O_{y-1}) + \textbf{E (TiO)} - \textbf{E } (Ti_xO_y) \qquad \textbf{(4)}$$

Both in case of neutral and cationic clusters the TiO removal energy is higher for Ti_xO_{2x} cluster series than Ti_xO_{2x+1} cluster series indicating that Ti_xO_{2x} series is more stable than Ti_xO_{2x+1} series. If we look at the mass spectra we see that the intensity of $Ti_2O_4^+$ is higher than $Ti_2O_5^+$ and intensity of $Ti_3O_5^+$ is higher than $Ti_3O_6^+$ cluster. TiO removal energy criterion is also flawed as it compares only two series not all three of them.

(5) **Binding Energy / Atom:** Fig (3.10) & (3.11) below show the binding energy per atom for neutral and cationic Ti_xO_y clusters. In case of neutral clusters the binding energies are almost same for Ti_3O_6 and Ti_3O_5, Ti_4O_8 and Ti_4O_7, Ti_5O_9 and Ti_5O_{10}, indicating that these clusters are more stable than the other members of the series. But in case of cations the binding energy per atom is highest in the Ti_xO_{2x-1} cluster series, indicating that Ti_xO_{2x-1} is most stable followed by Ti_xO_{2x} and Ti_xO_{2x+1} cluster series. From the plot we can see that the binding energy/ atom for $Ti_2O_4^+$ cluster is greater than $Ti_2O_5^+$ cluster, suggesting that $Ti_2O_4^+$ is more stable than $Ti_2O_5^+$ cluster. But if we look at the mass spectra the intensity peak for $Ti_2O_5^+$ is higher than $Ti_2O_4^+$ cluster. This shows that the criterion of binding energy/ atom can be used to compare the stability of three different neutral and cationic Ti_xO_y cluster series but it does not tell us the whole story.

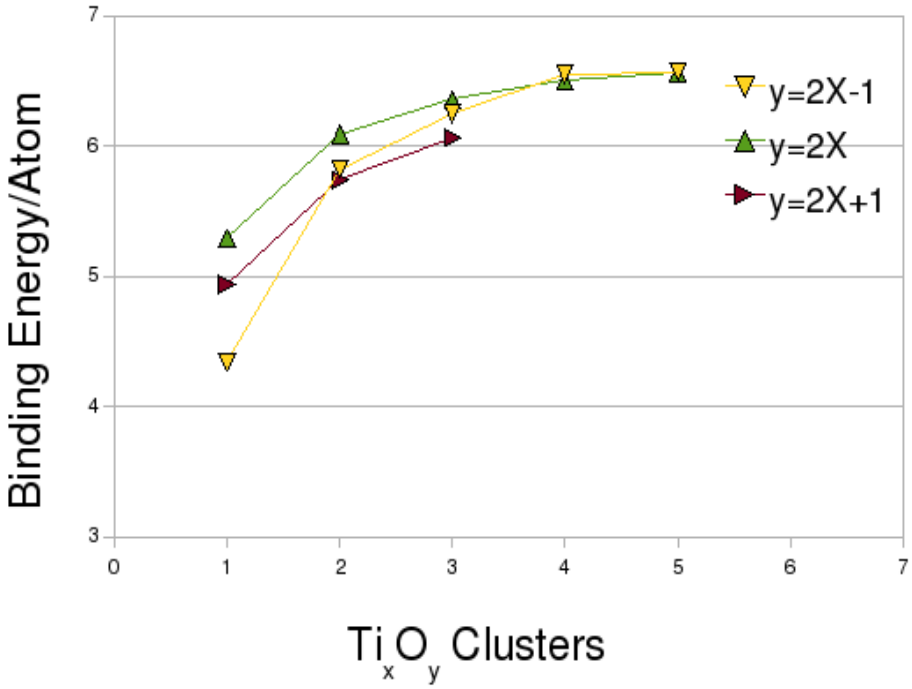

Fig.(3.10) Binding Energy per atom for Ti_xO_y clusters

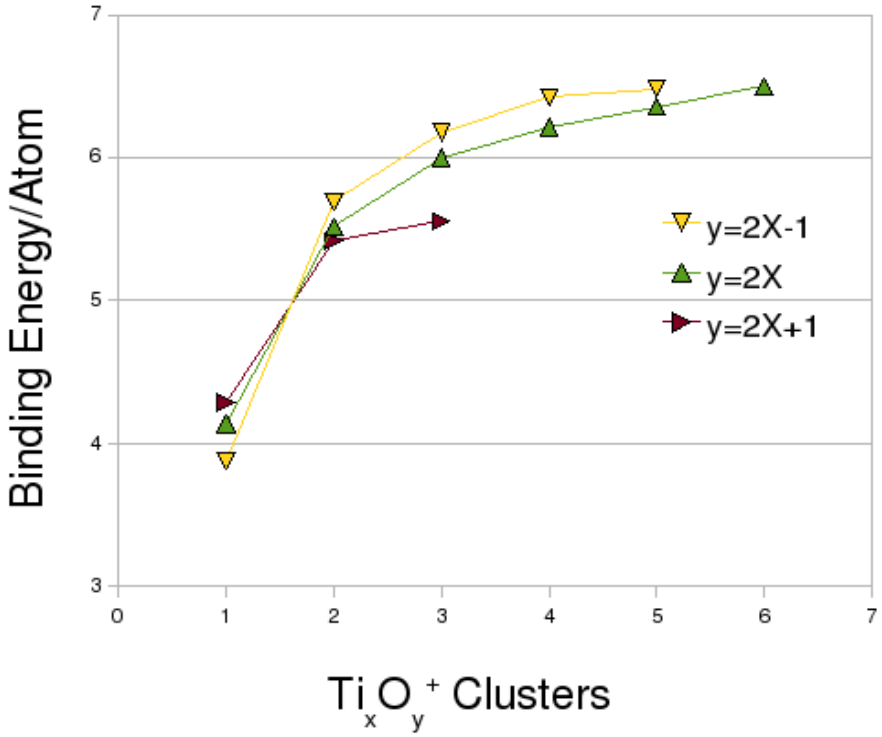

Fig.(3.11) Binding Energy per atom for Ti_xO_y $^+$clusters

Let us do the more specific comparison of the binding energy /atom for clusters having same number of Ti atom and different number of O atom. Fig (3.12) shows the Binding energy/ atom for Ti_3O_x clusters where x = 3 – 7.

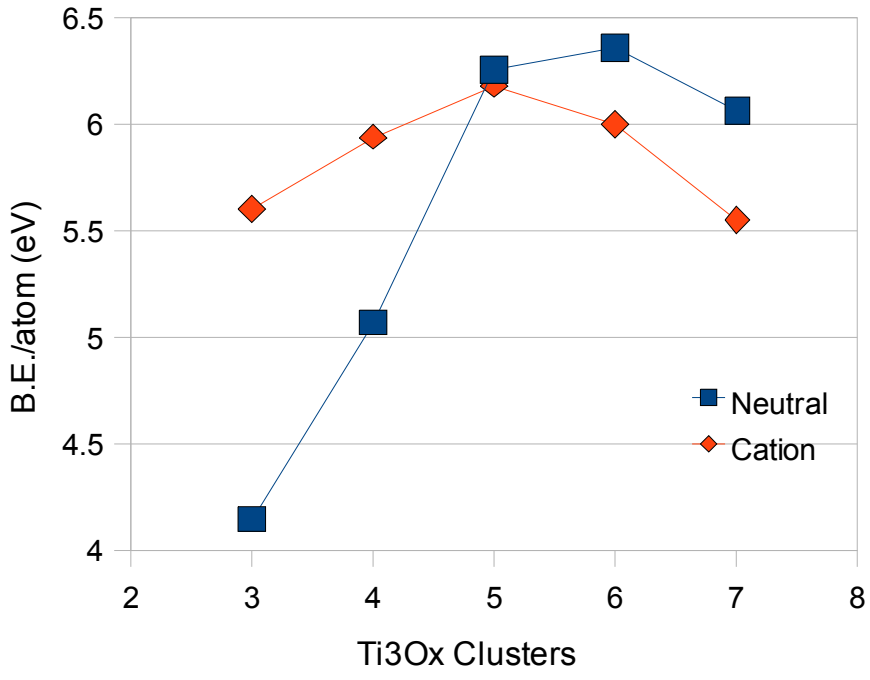

Fig.(3.12) Binding Energy per atom for Ti_3O_x clusters

As clear from the Fig above, in case of neutral clusters the Binding energy / atom is highest in case of Ti_3O_6 and it decreases with the addition and removal of one oxygen atom, indicating that Ti_3O_6 is most stable. Where as in case of cationic clusters the binding energy/atom increases as we move from x =3 -5 , ,indicating that $Ti_3O_5^+$ is most stable in the series followed by $Ti_3O_4^+$ and $Ti_3O_3^+$. This is clearly seen in the mass spectra where the peak is highest at $Ti_3O_5^+$. Also as we move to $Ti_3O_6^+$ and $Ti_3O_7^+$ we see there is a drop in Binding energy / atom, indicating less stability of these clusters as compared to $Ti_3O_5^+$.

(6) **HOMO-LUMO gap:** Fig (3.13) below show the HOMO – LUMO gap for the neutral clusters.

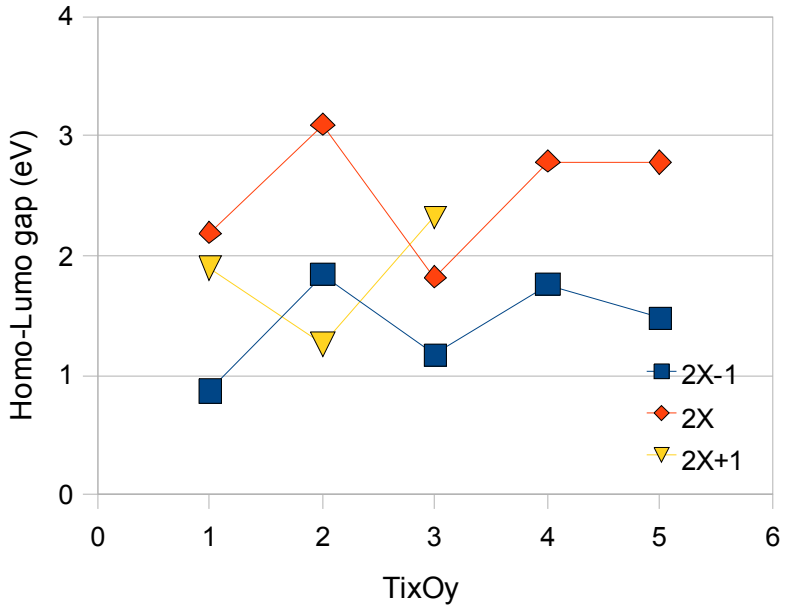

Fig (3.13): HOMO – LUMO gap in Ti_xO_y clusters

As shown in the fig above the HOMO-LUMO gap is smaller in case of 2x-1 series indicating that this series is probably more reactive and has a low ionization potential and thus is unstable as neutral so it preferably stays as cations. On the other hand 2x series shows the largest HOMO-LUMO gap, and thus generally will have a higher ionization potential, and that is why we expect Ti_xO_{2x} neutral clusters series to be the most stable, and least stable as cations as seen in the mass spectra is lowest.

From the above six criterion, the ionization potential is the most reliable one to identify the stability of cationic clusters. This is not unusual for mass spectra in which no etching is performed, and in which the clusters are "hot", in which the LaVa plasma is allowed to

expand into a vacuum without completely cooling. The second more reliable criterion is HOMO-LUMO gap .The other criterion like TiO and oxygen removal energy and TiO_2 removal are not so accurate to describe the stability of three different Ti_xO_y clusters. However binding energy/atom also yields the reliable results but it does show some discrepancies in the results.

Next, to understand the origin of the stability and especially the low ionization potential of the Ti_xO_{2x-1} clusters, we now examine the electronic structure of several representative clusters. First we look at the absolute value of the HOMO and LUMO of the clusters to determine their tendency to donate or accept charge. A plot of the absolute value of HOMO and LUMO for the Ti_3O_x neutral cluster series where x =3-7, is shown below in Fig (3.14).

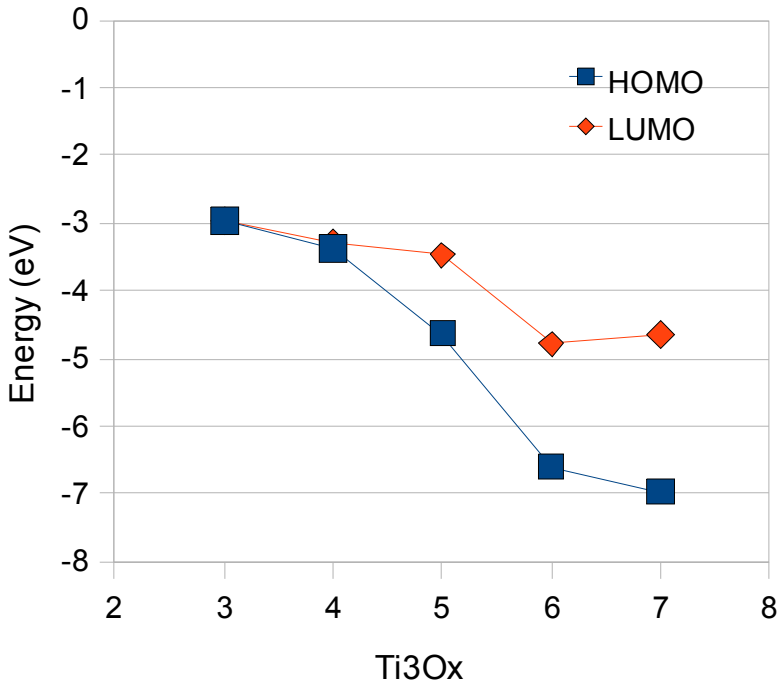

Fig(3.14) Absolute value of HOMO- LUMO for the Ti_3O_x clusters

We see that Ti_3O_3, Ti_3O_4 and Ti_3O_5 have high lying HOMOs which explain their small ionization potential, indicating that these clusters have tendency to give up electrons and are more likely to prefer to stay as cations. On the other hand Ti_3O_6 and Ti_3O_7 clusters have low lying HOMO and thus possess high ionization potential, indicating that these clusters do not want to give up electrons and are more stable as neutrals.

To examine the electronic structure more carefully, we next look at the density of states of Ti_3O_5 and Ti_3O_6. The total density of states is in black, Ti is in blue, O is in red, and Ti(D) is in purple. The HOMO of Ti_3O_6 is particularly lying at oxygen. Ti_3O_6 has a large HOMO-LUMO gap and a small gap between HOMO/HOMO-1. As we can see from Fig (1.5) for Ti_3O_6 we have one filled state at the Fermi level followed by a couple of state that are less than 1eV lower in energy. In Ti_3O_5, the HOMO is particularly lying at Ti. Whereas in case of the Ti_3O_5, the gap between the HOMO and HOMO-1 is about 2eV. This high lying HOMO suggests Ti_3O_5 is electronically more stable. This states why the HOMO is so high in energy in Fig.(3.14), and this is what causes the Ti_3O_5, and 2x-1 series to prefer to be cations.

To confirm this, we next examine the density of states for Ti_3O_5 and Ti_3O_6 as shown in Fig.(3.15) and the same for their cations $Ti_3O_5^+$ and $Ti_3O_6^+$ in Fig.(3.16). It is clear form Fig.(3.16) that $Ti_3O_6^+$ has LUMO (or SUMO – Singly Unoccupied Molecular Orbit) which is 0.5 eV above the Fermi energy, followed by a large gap. This confirms that $Ti_3O_6^+$ would like an additional electron for maximum electronic stability. In case of $Ti_3O_5^+$, there is still a large HOMO HOMO-1 gap, however it is only in the alpha spin channel. This indicates that

the cluster would like to lose one more electron for maximum electronic stability suggesting that $Ti_3O_5^+$ is more stable as a cation than $Ti_3O_6^+$.

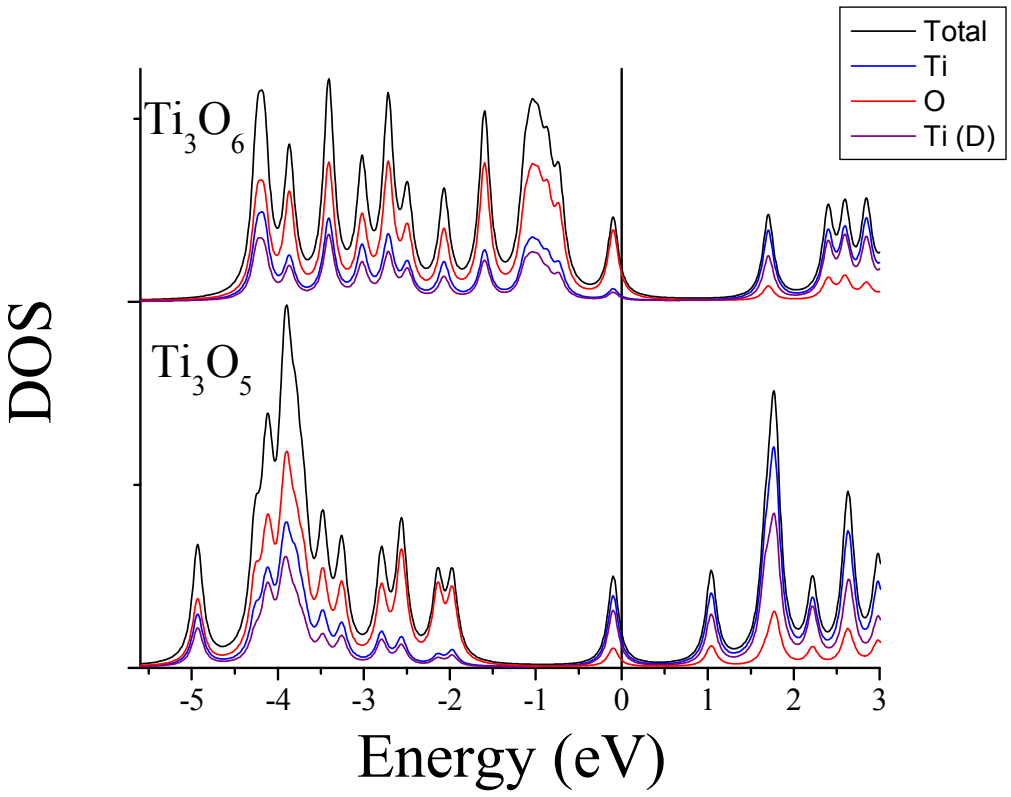

Fig.(3.15) Density of States of the neutrals 35 and 36. Broadening is done using Lorentzians with a width of 0.075 eV.

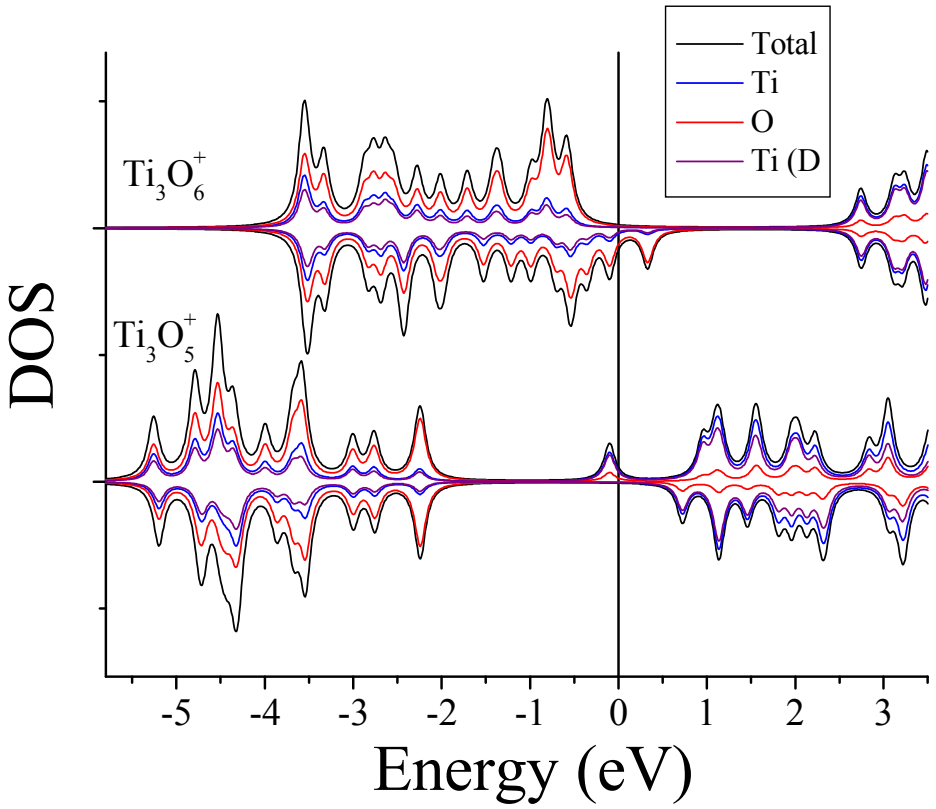

Fig.(3.16) Density of States of the cations 35 and 36. Broadening is done using Lorentzians with a width of 0.075 eV.

Chapter 4: Conclusions

4.1 Summary

The electronic structure and the stability of neutral and cationic Ti_xO_y clusters with x = 1-5 (where y =2x-1, 2x and 2x+1) have been investigated using the Density functional theory within NRLMOL code. The cationic clusters keep the same geometries as their neutral parents, with small changes in bond lengths and bond angles. Oxygen generally prefers to be divalent but as the Ti_xO_y clusters as the cluster size increases oxygen atom exhibits trivalent and tetravalent character. In Ti_xO_y cluster series, as we move from x =1 to 5, the corresponding geometries also changes from linear to rhombic to hexagonal and finally we get a cage like structure for the higher members. The low lying structures for x=3-5 usually show one or two terminal Ti-O bonds of constant length.

Bulk titanium-oxide, and nanoparticles of TiO are found to have the stoichometry of Ti_xO_{2x}, but for $Ti_xO_y^+$ clusters 2x-1 series is relatively more stable. To understand the origin of the stability of the $Ti_xO_{2x-1}^+$ clusters, we used different analyzing factors like ionization potential, TiO_2 removal energy, oxygen removal energy, Binding energy per atom and HOMO-LUMO gap. After analyzing the above different criterion we find out that the ionization potential and HOMO-LUMO gap provides the best criterion to explain the stability of $Ti_xO_{2x-1}^+$ clusters. The low ionization potential and HOMO-LUMO gap of 2x-1 series generally suggests that these clusters would more likely prefer to stay as cations. To examine the electronic structure more carefully, we next looked at the density of states of

Ti_3O_5 and Ti_3O_6. In the case of Ti_3O_5, there is a large HOMO HOMO-1 gap, indicates that the cluster would like to lose one more electron for maximum electronic stability and this is what causes the Ti_3O_5, and 2x-1 series to prefer to be cations.

References

1. Castleman, A. W., Jr.; Khanna, S. N. *J. Phys. Chem. C* **2009**, *113*, 2664.
2. Jena, P.; Castleman, A. W., Jr. *Proc. Natl. Acad. Sci. U.S.A.* **2006**, *103*, 10560.
3. Bergeron, D. E.; Roach, P. J.; Castleman, A. W., Jr.; Jones, N. O.; Khanna, S. N. *Science* **2005**, *307*, 231.
4. W. A. de Heer, Rev. Mod. Phys. 65, 611 (1993).
5. P. Clayborne, N.O. Jones, A.C. Reber, J.U. Reveles, M. Qian, and S.N. Khanna. J. Comp. Meth. Sci. Eng. **7**, 417 (2007).
6. M. Foltin, G.J. Stueber, E.R. Bernstein, J. Chem. Phys. **111**, 9577 (1999)
7. Z.-W. Qu, G.-J. Kroes, J. Phys. Chem. B **110**, 8998 (2006)
8. J. Xiang, X.H. Yan, Y. Xiao, Y.L. Mao, S.H. Wei, Chem. Phys. Lett. **387**, 66 (2004)
9. J.E. Huheey, *Inorganic Chemistry: Principles of Structure and Reactivity*, 2nd edn. (Harper and Row, New York, 1978).
10. Z-w. Qu, and G-J. Kroes, J. Phys. Chem. C 111, 16808 (2007)
11. H. Wu, L-S. Wang, J. Chem. Phys. 107, 8221 (1997)
12. K. S. Jeong, Ch Chang, E. Sedlmayr, and D. Sülzle, J. Phys. B 33, 3417 (2000).
13. H-J. Zhai, and L-S. Wang, J. Am. Chem. Soc. 129, 3022 (2007).
14. M. Calatayud, L. Maldonado, and C. Minot J. Phys. Chem. C 112, 16087 (2008)
15. S. Li, and D. A. Dixon, J. Phys. Chem. A 112, 6646 (2008)

16. Y. Liu, Y. Yuan, Z. Wang, K. Deng, and C. Xiao, J. Chem. Phys. 130, 174308 (2009)

17. X.H. Liu, X.G. Zhang, Y. Li, X.Y. Wang, N.Q. Lou, Int. J. Mass Spectrom. **177**, L1 (1998).

18. T. Albaret, F. Finocchi, C. Noguera, J. Chem. Phys. **113**, 2238 (2000)

19. Ch. Lüder, E. Georgiou, M. Velegrakis, Int. J. Mass. Spectrom. Ion Proc. **153**, 129 (1996).

20. J. Giapintzakis, A. Sfounis, M. Velegrakis, Int. J. Mass. Spectrom. Ion Proc. **189**, 1 (1999)

21. M. Velegrakis, A. Sfounis, Appl. Phys. A 97, 765 (2009).

22. W. Yu, R.B. Freas, J. Am. Chem. Soc. 112, 7126 (1990).

23. Z.-W. Qu, G.-J. Kroes, J. Phys. Chem. B **110**, 8998 (2006).

24. A. Hagfeldt, R. Bergstrom, H.O.G. Siegbahn, S. Lunell, J. Phys. Chem. **97**, 12725 (1993).

25. X. Matsuda, E.R. Bernstein, J. Phys. Chem A **109**, 314 (2005).

26. Elementary quantum chemistry, Frank L. Pilar.

27. K. Capelle, Brazilian Journal of Physics, 36, 1318 (2006).

28. Electronic Structure: Basic Theory and Practical Methods, R. M. Martin, Cambridge University Press, NY, 2006.

29. Pederson, M. R.; Jackson, K. A. *Phys. Re*V. *B* **1990**, *41*, 7453.

30. Jackson, K.; Pederson, M. R. *Phys. Re*V. *B* **1990**, *42*, 3276.

31. Porezag, D.; Pederson, M. R. *Phys. Re*V. *A* **1999**, *60*, 2840.